



# Influence of Heat and Mass Transfer on Free Convection of Micropolar Fluid between Vertical Concentric Cylinders

A. K. Singh and A. K. Singh

*Department of Mathematics, Institute of Science, Banaras Hindu University, Varanasi-221005, India*

†Corresponding Author Email: [arunsingh253@gmail.com](mailto:arunsingh253@gmail.com)

(Received March 24, 2018; accepted December 12, 2018)

## ABSTRACT

Natural convective flow of a micropolar fluid is examined analytically in order to see the effect of heat and mass transfer between two concentric vertical cylinders of infinite length. The governing equations of model in non-dimensional form corresponding to the temperature, velocity and microrotational velocity, using the Boussinesq approximation and Eringen equation with suitable boundary conditions are expressed in terms of cylindrical coordinate system and then their exact solutions are obtained. The influence of the non-dimensional physical parameters such as the material and vortex viscosity parameters on the velocity, microrotational velocity is evaluated by showing on the graphs while the values of skin friction in non-dimensional form at the outer and inner surfaces of inner and outer cylinders have been presented in the tabular form.

**Keywords:** Micropolar fluid; Natural convection; Temperature; Two concentric vertical cylinders.

## NOMENCLATURE

$a$	radius of the inner cylinder	$\alpha, \beta, \lambda'$	spin vector
$b$	radius of the outer cylinder	$\beta'$	coefficient of thermal expansion
$B$	material parameter	$\gamma$	spin-gradient viscosity
$f$	body force vector	$\kappa$	vortex viscosity coefficient
$g$	acceleration due to gravity	$\lambda$	ratio of outer radius and inner radius
$j$	micro inertia density per unit mass	$\mu$	shear viscosity coefficient of fluid
$m$	temperature ratio parameter	$\rho$	density of fluid
$N_u$	Nusselt number	$\tau$	dimensionless Skin friction coefficient
$q$	heat flux	$\tau_1$	skin friction at the outer surface of inner cylinder
$R$	vertex viscosity ratio parameter	$\tau_\lambda$	Skin friction at the inner surface of outer cylinder
$r'$	transverse coordinate	$\vec{\omega}$	micro-rotation vector
$r$	dimensionless transverse coordinate	$\omega'$	microrotational (Angular) velocity
$T'$	temperature of the fluid	$\omega$	dimensionless Microrotational velocity
$T$	dimensionless temperature	$\Phi$	mechanical energy/mass
$u'$	stream wise velocity		
$u$	dimensionless stream wise velocity		
$\vec{V}$	velocity vector		

## 1. INTRODUCTION

The physical characteristics of many fluids flows can't be successfully presented by the Navier–Stokes equations for the Newtonian fluids because they have behaviors like non-Newtonian fluids. From which, micropolar fluid may be considered as a non-Newtonian fluid having of short rigid

cylindrical element or dumb-bell molecules, polymer solutions, colloidal suspensions etc. The micro-structure of fluid particles in a viscous medium is displayed as being rigid and randomly spheroidal arranged where the distortions of these fluids are disregarded. Also, the theory of a micropolar fluid is described to find the kinematics of micro-rotation with velocity, angular velocity and some parameters. The mathematical modeling

of micropolar fluid has been introduced by Eringen (1966) which shows the impact of the couple stress tensor and the body couple. Some authors explained different physical properties and also given different governing equations for the non-Newtonian fluids. Ariman *et al.* (1973) have presented the most important reviews about microcontinuum fluid mechanics which is favorable conditions for many non-Newtonian fluids. Using micropolar fluid model, research workers can describe the physical characteristic of some non-Newtonian fluids such as animal blood and liquid crystals, clouds with smoke, certain polymer solutions, ferro liquids, complex biological structures, colloidal suspensions, lubricating fluids etc. Gorla and Ameri (1985) have derived the solution of a micropolar fluid along a continuous and moving cylinder with the suitable boundary layer problem. Bhattacharyya and Pop (1996) have employed the model of a micropolar fluid described by Eringen to calibrate the natural convective flow in cylinders having the elliptic cross-section. Singh *et al.* (1997) have examined free convective flow of a fluid between two vertical concentric annuli, with radial magnetic field by obtaining the analytic solution for the problem. Using the Eringen models, Char and Lee (1998) have explained in details the free convective flow of a micropolar fluid between horizontal eccentric cylinders with maximum density. Mrabti *et al.* (2000) have analyzed the impacts of micro-structure on free convection of a micropolar fluids in a vertical cylinder when it is heated from below. Lukaszewicz (2003) has studied the asymptotic behavior of a micropolar fluid flow having some symmetries. Srinivasacharya *et al.* (2003) have described the Peristaltic pumping of an incompressible micropolar fluid with long wavelength in a circular tube. Using the rotary oscillations around a common diameter, Iyengar and Vani (2004) have conducted a systematic study of an incompressible micropolar fluid flow, within two concentric spheres. Aydin and Pop (2005) have examined the influence of the parameters such as the length of the isoflux discrete heater, material parameter, Prantl number as well as the Rayleigh number on the free convective flow of a micropolar fluid. The study of momentary natural convection of a micropolar fluid between concentric and eccentric spheres has been performed numerically by Chen (2005). Ishak *et al.* (2006) have obtained the solution of the problem of steady and laminar forced convection of a micropolar fluid along moving wedge and also on a flat plate. In particular, this author has introduced the physical properties of a micropolar fluid on the walls of the wedge having suitable boundary-layer. Muthu *et al.* (2008) have discussed the flow of a micropolar fluid in a catheterized artery having application to blood flow. Also, the influences of catheter size on the wall shear stress are given.

Further, Alloui and Vasseur (2010) have demonstrated numerically using control volume approach and SIMPLER algorithm (Patankar, 1980) free convection of a micropolar fluid,

within a shallow rectangular cavity. This problem has been discussed in details through numerical solution corresponding to the material parameter, the thermal Rayleigh number and microrotation boundary condition. Ravi *et al.* (2011) have reported the impact of parameters related to natural convection of a micropolar fluid within two vertical walls in presence of the temperature dependent source/sink. Chen *et al.* (2012) have studied the unsteady flow of a compressible micropolar fluid numerically applying the spectral difference method and demonstrated the numerical results in the case of Couette flow. Bourantas and Loukopoulos (2014) have introduced the theory of the natural convective flow of a micropolar nanofluids in a square cavity. The influence of the transient buoyancy-opposed double diffusive free convection of a micropolar fluids within a square enclosure has been described by Jena *et al.* (2015). More recently, the impact of non-uniform heat source on free convective flow of a micropolar fluid have been considered by Muthamilselvan *et al.* (2017). Sheremet *et al.* (2017) have described the impact of time-dependent free convective flow of a micropolar fluid in a wavy triangular cavity. Singh and Singh (2017 a, b) have studied the influences of non-dimensional physical parameters concerned with the models on the velocity and microrotational velocity with natural convection of a micropolar in two vertical wall and and polar fluid in the concentric cylinders respectively. Using the Faedo–Galerkin method, Drazic *et al.* (2017) have used the numerical solution to study the flow of a compressible and viscous micropolar fluid between two coaxial cylinders.

In the present paper, we analyse the free convection of a micropolar fluid between two vertical concentric cylinders with the Dirichlet boundary conditions. We solve the governing simultaneous differential equations and obtain the solution for the angular velocity and velocity. At last, using the graphs and table, we have shown the impact of the temperature ratio ( $m$ ), vertex viscosity ratio, radii ratio (gap between the two vertical concentric cylinders) and material parameters on the skin friction, velocity as well as microrotational velocity.

## 2. MATHEMATICAL FORMULATIONS

By using the Eringen theory, the governing simultaneous differential equations for the steady free convective flow of a micropolar fluid in the vector form are as follows:

Conservation of mass

$$\nabla \cdot \vec{V} = 0, \quad (1)$$

Conservation of linear momentum

$$0 = -\nabla p + \kappa \nabla \times \vec{\omega} + (\mu + \kappa) \nabla \times \nabla \times \vec{V} + (\lambda + 2\mu + k) \vec{V} + \rho \vec{g}, \quad (2)$$

Conservation of angular momentum

$$0 = \kappa \nabla \times \vec{V} - 2\kappa \vec{\omega} + \gamma (\nabla \times \nabla \times \vec{\omega}) + (\alpha + \beta + \lambda) \nabla (\nabla \cdot \vec{\omega}), \quad (3)$$

Conservation of thermal Energy

$$0 = -\rho \nabla \cdot \vec{V} + \rho \Phi - \nabla \cdot q, \quad (4)$$

where  $\gamma = (\mu + 0.5\kappa)j$  and

$$\rho \Phi = \lambda (\nabla \cdot \vec{V})^2 + 2\mu D : D + 4k \left( \frac{1}{2} \nabla \times \vec{V} - \vec{\omega} \right)^2 + \alpha (\nabla \cdot \vec{\omega})^2 + \gamma \nabla \vec{\omega} : \nabla \vec{\omega} + \beta \nabla \vec{\omega} : (\nabla \vec{\omega}). \quad (5)$$

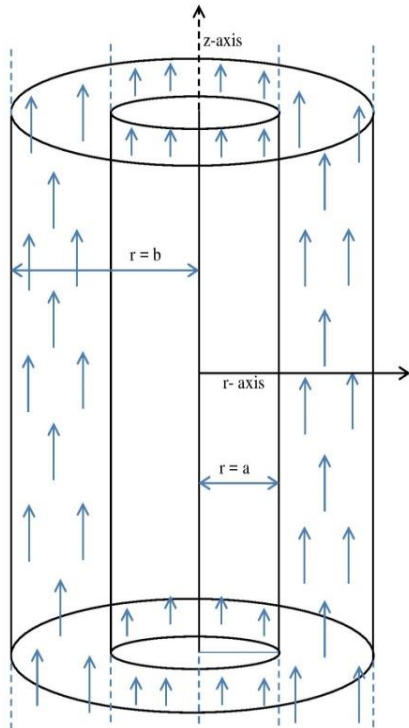


Fig. 1. Physical model.

Here, we have taken the steady and laminar free convection of a micropolar fluid in two infinite vertical and concentric cylinders as explained in Fig. 1. The axes of cylinders are taken along the  $z'$ -axis in the vertical upward direction and its radial direction is the  $r'$ -axis. Let  $a$  and  $b$  are radii of inner and outer cylinders, and having asymmetric temperature  $T'_1$  and  $T'_2$  respectively. Since the length of the cylinders is infinite, the flow is fully developed and is depending only on the coordinate  $r'$ . The governing differential equations for the free convective flow of a micropolar fluid are derived by applying the Boussinesq approximation and they are obtained as follows:

$$(\mu + \kappa) \frac{1}{r'} \frac{d}{dr'} \left( r' \frac{du'}{dr'} \right) + \kappa \left( \frac{\omega'}{r'} + \frac{d\omega'}{dr'} \right) + \rho g \beta' (T' - T'_0) = 0, \quad (6)$$

$$\gamma \left[ \frac{1}{r'} \frac{d}{dr'} \left( r' \frac{d\omega'}{dr'} \right) - \frac{\omega'}{r'^2} \right] - \kappa \left( \frac{du'}{dr'} + 2\omega' \right) = 0, \quad (7)$$

$$\frac{1}{r'} \frac{d}{dr'} \left( r' \frac{dT'}{dr'} \right) = 0. \quad (8)$$

The applicable boundary conditions for the considered physical model are:

$$\begin{aligned} u' = 0, \quad \omega' = 0, \quad T' = T'_1, \quad \text{at } r' = a, \\ u' = 0, \quad \omega' = 0, \quad T' = T'_2, \quad \text{at } r' = b. \end{aligned} \quad (9)$$

In order to non-dimensionalise the model equations, we use the following non-dimensional variables:

$$\begin{aligned} u = u' \mu \left[ \beta' g a^2 (T' - T'_0) \right]^{-1}, \quad B = \frac{a^2}{j}, \quad r = \frac{r'}{a}, \\ \omega = \omega' \mu \left[ \beta' g a^2 (T' - T'_0) \right]^{-1}, \quad T = \frac{(T' - T'_0)}{(T'_1 - T'_0)}, \\ m = \frac{(T'_2 - T'_0)}{(T'_1 - T'_0)}, \quad \lambda = \frac{b}{a}, \quad R = \frac{k}{\mu}. \end{aligned} \quad (10)$$

After substituting Eq. (10) into Eqs. (6) - (9), the governing equations and boundary conditions of the present problem become in non-dimensional form became

$$(1 + R) \left[ \frac{d^2 u}{dr^2} + \frac{1}{r} \frac{du}{dr} \right] + R \left[ \frac{\omega}{r} + \frac{d\omega}{dr} \right] + T = 0, \quad (11)$$

$$(1 + 0.5R) \left[ \frac{d^2 \omega}{dr^2} + \frac{1}{r} \frac{d\omega}{dr} - \frac{\omega}{r^2} \right] - BR \left( \frac{du}{dr} + 2\omega \right) = 0, \quad (12)$$

$$\frac{d^2 T}{dr^2} + \frac{1}{r} \frac{dT}{dr} = 0, \quad (13)$$

with the boundary conditions as:

$$\begin{aligned} u = 0, \quad \omega = 0, \quad T = 1, \quad \text{at } r = 1, \\ u = 0, \quad \omega = 0, \quad T = m, \quad \text{at } r = \lambda. \end{aligned} \quad (14)$$

### 3. SOLUTION

Governing non-dimensional differential Eqs. (11) to (13) along with its boundary conditions given in Eq. (14) are solved by applying the analytic method. First, Singh *et al.* (1997) have found the analytic result of thermal energy Eq. (13) with the boundary condition, which is as follows:

$$T = P_1 \log r + 1. \quad (15)$$

Putting above expression of temperature (T) in Eq. (11) and then we can rewrite this equation in the form:

$$\frac{d}{dr} \left[ (1 + R) r \frac{du}{dr} + R \omega r \right] = -(P_1 \log r + 1) r. \quad (16)$$

Integrating (16) w. r. t.  $r$  and then dividing by  $r$ , we obtain

$$\frac{du}{dr} = -\frac{r}{2}P_2 \left[ P_1 \left( \log r - \frac{1}{2} \right) + 1 \right] + \frac{P_2 C_1}{r} - RP_2 \omega. \quad (17)$$

Using (17) into (12), we obtain

$$\frac{d^2 \omega}{dr^2} + \frac{1}{r} \frac{d\omega}{dr} - \left( P_4^2 + \frac{1}{r^2} \right) \omega = \frac{P_2}{P_3} \left[ -P_1 \frac{r}{2} \left( \log r - \frac{1}{2} \right) - \frac{r}{2} + \frac{C_1}{r} \right]. \quad (18)$$

The general solution of (18) is obtained as

$$\omega = C_3 I_1(P_4 r) + C_2 K_1(P_4 r) + P_7 r \log r + P_{10} r + \frac{-2C_1 P_8}{r} + \frac{P_9}{r}. \quad (19)$$

In above equation,  $I_1(P_4 r)$  and  $K_1(P_4 r)$  are modified Bessel functions of first order of first and second kind. Putting Eq. (19) into Eq. (17) and integrating, we get:

$$u = P_{20} C_3 I_0(P_4 r) - P_{20} C_2 K_0(P_4 r) + P_{21} r^2 \log r + P_{22} r^2 + P_{19} C_1 \log r + P_{16} \log r + C_4, \quad (20)$$

where  $I_0(P_4 r)$  and  $K_0(P_4 r)$  are modified Bessel functions of zero order. Using the boundary conditions given in Eq. (14) into Eqs. (19) and (20), we obtain the arbitrary constant  $C_1, C_2, C_3$  and  $C_4$ . The solutions for the velocity and microrotational velocity are given by

$$u = P_{51} P_{20} I_0(P_4 r) - P_{52} P_{20} K_0(P_4 r) + (P_{21} r^2 + P_{19} P_{50} + P_{16}) \log r + P_{22} r^2 + P_{53}, \quad (21)$$

$$\omega = P_{51} I_1(P_4 r) + P_{52} K_1(P_4 r) + P_7 r \log(r) + P_{10} r + \frac{(P_9 - 2P_8 P_{50})}{r}. \quad (22)$$

$P_1, P_2, P_3, \dots, P_{53}$ , used in above equations are defined in appendix. Using Eq. (21), we have evaluated the skin-frictions for the natural convection of a micropolar fluid at the surface of the cylinders which are as follow:

$$\tau_1 = \left( \frac{du}{dr} \right)_{r=1} = P_{51} P_{12} I_1(P_4) + P_{52} P_{12} K_1(P_4) + P_{54}, \quad (23)$$

$$\tau_\lambda = \left( \frac{du}{dr} \right)_{r=\lambda} = P_{51} P_{12} I_1(P_4 \lambda) + P_{52} P_{12} K_1(P_4 \lambda) + P_{55}. \quad (24)$$

#### 4. RESULTS AND DISCUSSION

In the above section, we have obtained analytical solution of the governing differential equations describing the free convection of a micropolar fluid between two vertical and concentric cylinders. In

this section, we describe the influences of dimensionless physical parameters such as the temperature ratio ( $m$ ), material number ( $B$ ) and vertex viscosity ratio ( $R$ ) on the velocity and angular velocity by using the graphs. It should be noted that the values of the temperature ratio parameter  $m = 1$  and  $m = 0$  are corresponding to the symmetric and asymmetric cases respectively. When the vertex viscosity ratio parameter  $0 < R = \frac{\kappa}{\mu} < 1$ , the shear viscosity coefficient ( $\mu$ ) is greater than the vortex viscosity (micro-rotation viscosity) coefficient  $k$  while converse trend occurs when  $R = \frac{\kappa}{\mu} > 1$ .

Graphical representation in Figs. 2 and 3 shows the effect of the material and vertex viscosity ratio parameters on the velocity corresponding to temperature ratio parameter  $m = 0$  and  $m = 1$  respectively. Comparison of these figures clearly indicates that the velocity of micropolar fluids is more in case of symmetric heating. When the vertex viscosity ratio increases, the velocity of the fluid decreases while the reverse phenomenon occurs when the material number increases for both cases of asymmetric and symmetric heating. The rate of decreasing velocity is greater for the vertex viscosity ratio  $0 < R < 1$  compared to the vertex viscosity ratio  $R > 1$  with both cases of the asymmetric ( $m = 0$ ) and symmetric ( $m = 1$ ) heating.

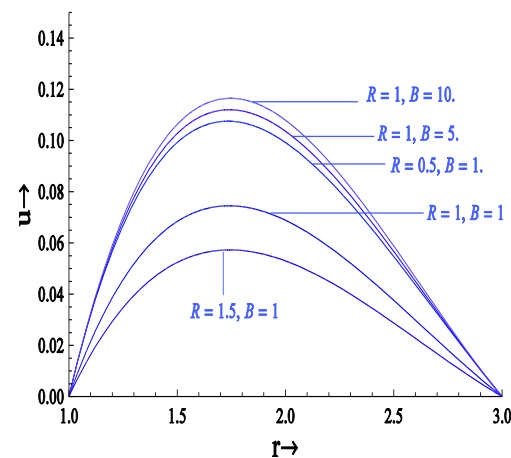


Fig. 2. Variation of velocity for  $m=0$ .

Figures 4 and 5 reveal the variation of the angular velocity with the material number and vertex viscosity ratio parameters, corresponding to temperature ratio  $m = 0$  and  $m = 1$  respectively. The angular velocity of a micropolar fluid is less in the case of asymmetric heating ( $m = 0$ ) compare to symmetric heating ( $m = 1$ ). When  $R > 1$ , the impact of the vertex viscosity ratio parameter is to decrease the angular velocity in the asymmetric and symmetric heating cases while converse trend occurs when  $0 < R < 1$ . The velocity of a micropolar fluid enhances with the material parameter in both cases of the asymmetric and symmetric temperature ratio. The rate of decreasing of microrotational velocity is faster for the vertex

viscosity ratio  $0 < R < 1$  compared to the vertex viscosity ratio  $R > 1$  with both case of the asymmetric and symmetric heating.

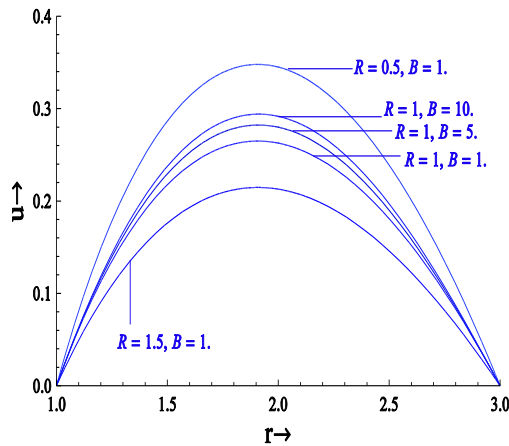


Fig. 3. Velocity profiles for  $m=1$ .

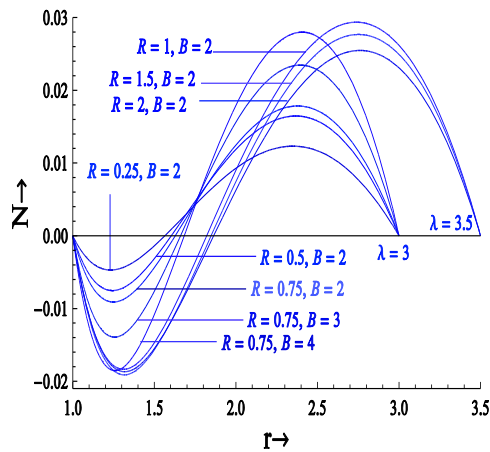


Fig. 4. Microrotational velocity for  $m=0$ .

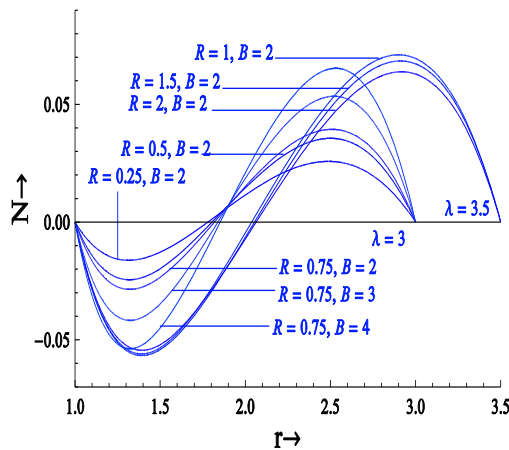


Fig. 5. Variation of microrotational velocity for  $m=1$ .

In Table 1, we have described the numerical values of the skin friction  $\tau_1$  and  $\tau_\lambda$  by varying the physical parameters such as the material, vertex viscosity ratio, temperature ratio and radii ratio parameters. The skin friction increases when the

material and the radii ratio (gap between the cylinders,  $\lambda$ ) parameters increase corresponding to temperature ratio parameters  $m=0$  and  $m=1$  respectively. For both cases  $m=0$  and  $m=1$ , the skin friction decreases when vertex viscosity ratio parameter increases. The decreasing rate of the skin friction is more for the vertex viscosity ratio parameter  $0 < R < 1$  compared to the vertex viscosity ratio parameter  $R > 1$ .

### CONCLUSION

In this paper, by using the analytic method, we have obtained the solution for the given problem of natural convection of a micropolar fluid in vertical and concentric annuli. We have explained the physical behavior of some parameters such as the vertex viscosity ratio, material parameters, temperature ratio and radii ratio parameters on the temperature, the velocity, the microrotational velocity as well as the skin friction. The following conclusions are derived as:

- An enhance in the vortex viscosity ratio is to decrease the velocity of fluids corresponding to both symmetric and asymmetric heating. The rate of decreasing velocity is less for the vortex viscosity ratio parameter  $R > 1$ , compared to the vortex viscosity ratio parameter  $0 < R < 1$ .
- When  $0 < R < 1$ , the microrotational velocity of fluids increases with the vortex viscosity ratio parameter for the asymmetric and symmetric cases while converse trends occur when  $R > 1$ .
- The velocity and microrotational velocity of a micropolar fluid is improving with the material parameter for asymmetric and symmetric temperature ratio.
- The effect of the material, temperature ratio and radii ratio parameters is to enhance the skin friction  $\tau_1$  and  $\tau_\lambda$  of a micropolar fluid. An enhance in the vertex viscosity ratio is to decrease the skin friction.

### ACKNOWLEDGMENTS

Author Arun Kumar Singh thankfully acknowledges the financial relief from UGC, New Delhi as a Junior Research Fellowship during this work.

### REFERENCES

Alloui, Z. and P. Vasseur (2010) Natural convection in a shallow cavity filled with a micropolar fluid, *International Journal of Heat and Mass Transfer* 53, 2750–2759.

Ariman, T., M. A. Turk and N. D. Sylvester (1973) Micro-continuum fluid mechanics—A review, *International Journal of Engineering Science* 11, 905-930.

**Table 1** Values of the skin-friction at inner surface of outer cylinder and outer surface of inner cylinder

$\lambda$	m	R	B	$\tau_1$	$\tau_\lambda$
2	0	0.5	1	0.226703	-0.080656
		0.5	2	0.226917	-0.080549
		0.5	3	0.227102	-0.080456
		1	1	0.170287	-0.060362
		1.5	1	0.136407	-0.048201
		2	1	0.113791	-0.040108
	1	0.5	1	0.388239	-0.305881
		0.5	2	0.388429	-0.305786
		0.5	3	0.388591	-0.305704
		1	1	0.291411	-0.229295
		1.5	1	0.233287	-0.183357
		2	1	0.194511	-0.152744
3	0	0.5	1	0.470247	-0.136991
		0.5	2	0.471599	-0.136240
		0.5	3	0.472463	-0.135952
		1	1	0.354669	-0.101857
		1.5	1	0.284942	-0.081083
		2	1	0.238207	-0.067318
	1	0.5	1	0.883178	-0.594496
		0.5	2	0.884810	-0.593952
		0.5	3	0.885809	-0.593619
		1	1	0.664838	-0.445054
		1.5	1	0.533353	-0.355549
		2	1	0.445383	-0.295984

Aydin, O. and I. Pop (2005) Natural convection from a discrete heater in enclosures filled with a micropolar fluid, *International Journal of Engineering Science* 43, 1409–1418.

Bhattacharyya, S. and I. Pop (1996) Free convection from cylinders of elliptic cross-section in micropolar fluids, *International Journal of Engineering Science* 34, 1301–1310.

Bourantas, G. C. and V. C. Loukopoulos (2014) Modeling the natural convective flow of micropolar nanofluids, *International Journal of Heat and Mass Transfer* 68, 35–41.

Char, M. I. and G. C. Lee (1998) Maximum density effects on natural convection of micropolar fluids between horizontal eccentric cylinders, *International Journal of Engineering Science* 36, 157–169.

Chen, J., C. Liang and J. D. Lee (2012) Numerical simulation for unsteady compressible micropolar fluid flow, *Computers and Fluids* 66, 1–9.

Chen, W. R. (2005) Transient natural convection of micropolar fluids between concentric and vertically eccentric spheres, *International Journal of Heat and Mass Transfer* 48, 1936–1951.

Dražić, I., N. Mujaković and N. Črnjaričić (2017) Three-dimensional compressible viscous micropolar fluid with cylindrical symmetry: Derivation of the model and a numerical solution, *Mathematics and Computers in Simulation* 140, 107–124

Erigen, A. C. (1966) Theory of micropolar fluids, *Journal of Mathematics and Mechanics*, 16, 1–18.

Gorla, R. S. R. and A. Ameri (1985) Boundary layer flow of a micropolar fluid on a continuous moving cylinder, *Acta Mechanica* 57, 202–214.

Ishak, A., R. Nazar and I. Pop (2006) Moving wedge and flat plate in a micropolar fluid, *International Journal of Engineering Science* 44, 1225–1236.

Iyengar, T. K. V. and V. G. Vani (2004) Oscillatory flow of a micropolar fluid generated by the rotary oscillations of two concentric spheres, *International Journal of Engineering Science* 42, 1035–1059.

Jena, S. K., L. K. Malla, S. K. Mahapatra and A. J. Chamkha (2015) Transient buoyancy-opposed double diffusive convection of micropolar fluids in a square enclosure, *International Journal of Heat and Mass Transfer* 81, 681–694.

Lukaszewicz, G. (2003) Asymptotic behavior of micropolar fluid flows, *International Journal of Engineering Science* 41,259–269.

Mrabti, A., K. Gueraoui, A. Hiji and O. Terhmina (2000) Effects of microstructure on natural convection flow of micropolar fluids in a vertical cylinder heated from below, *International Journal of Engineering Science* 38, 823–831.

Muthamilselvan, M., K. Periyadurai and D. H. Doh (2017) Effect of uniform and non-uniform heat source on natural convection flow of micropolar fluid, *International Journal of Heat and Mass Transfer* 115, 19–34.

Muthu, P., B. V. Rathish Kumar and Peeyush Chandra (2008) A study of micropolar fluid in an annular tube with application to blood flow, *Journal of Mechanics in Medicine and Biology* 8, 561–576.

Ravi, S. K., A. K. Singh and K. A. Alawadhi (2011) Effects of temperature dependent heat source/sink on free convective flow of a micropolar fluid between two vertical walls, *International Journal of Energy & Technology* 3(27), 1-8.

Patankar, S., Numerical Heat Transfer and Fluid Flow, Hemisphere, Washington, DC, 1980.

Sheremet, M. A., I. Pop and A. Ishak (2017) Time-dependent natural convection of micropolar fluid in a wavy triangular cavity, *International Journal of Heat and Mass Transfer* 105, 610–622.

Singh, A. K. and A. K. Singh (2017a) Effect of heat source/sink on free convective flow of a polar fluid between vertical concentric annuli. *Journal of Applied Mathematics and Physics* 5, 1750-1762.

Singh, A. K. and A. K. Singh (2017b) Natural convection of a micropolar fluid between two vertical walls with Newtonian heating/cooling and heat source/sink, *Applications of Fluid Dynamics, Lecture Notes in Mechanical Engineering* 145-157.

Singh, S. K., B. K. Jha, and A. K. Singh (1997) Natural convection in vertical concentric annuli under a radial magnetic field. *Heat and Mass Transfer* 32, 399-401.

Srinivasacharya, D., M. Mishra and A. R. Rao (2003) Peristaltic pumping of a micropolar

fluid in a tube, *Acta Mechanica* 161, 165–178.

### APPENDIX

$$P_1 = \frac{m-1}{\text{Log}[\lambda]}, P_2 = \frac{1}{1+R}, P_3 = \frac{2+R}{2BR},$$

$$P_4 = \left( \frac{1}{P_3} (2 - P_2 R) \right)^{\frac{1}{2}}, P_5 = \frac{P_2}{2P_3(P_4)^2},$$

$$P_6 = P_1(P_4)^2, P_7 = P_5P_6, P_8 = P_5(P_4)^2,$$

$$P_9 = 2P_1P_5, P_{10} = P_8 \left( \frac{-P_1}{2} + 1 \right), P_{11} = -P_1P_2,$$

$$P_{12} = -RP_2,$$

$$P_{13} = P_7P_{12}, P_{14} = P_{10}P_{12}, P_{15} = 2P_8P_{12},$$

$$P_{16} = P_9P_{12}, P_{17} = P_{13} + \frac{P_{11}}{2},$$

$$P_{18} = P_{14} - \frac{P_{11}}{4} - \frac{P_{11}}{2}, P_{19} = P_2 - P_{15}, P_{20} = \frac{P_{12}}{P_4},$$

$$P_{21} = \frac{P_{17}}{2}, P_{22} = \frac{P_{18}}{2} - \frac{P_{17}}{4},$$

$$P_{23} = P_{20}\text{BesselI}(0, P_4), P_{24} = P_{20}\text{BesselK}(0, P_4),$$

$$P_{25} = P_{20}\text{BesselI}(0, P_4\lambda),$$

$$P_{26} = P_{20}\text{BesselK}(0, P_4\lambda),$$

$$P_{27} = P_{21}\lambda^2 \log\lambda + P_{22}\lambda^2 + P_{16}\log\lambda, P_{28} = P_{19}\log\lambda,$$

$$P_{29} = \text{BesselI}(1, P_4), P_{30} = \text{BesselK}(1, P_4),$$

$$P_{31} = P_9 + P_{10}, P_{32} = -2P_8, P_{33} = \text{BesselI}(1, P_4\lambda),$$

$$P_{34} = \text{BesselK}(1, P_4\lambda), P_{35} = P_7\lambda \log\lambda + P_{10}\lambda + \frac{P_9}{\lambda},$$

$$P_{36} = -\frac{2P_8}{\lambda}, P_{37} = \frac{P_{23} - P_{25}}{P_{24} + P_{26}}, P_{38} = \frac{P_{22} - P_{27}}{P_{24} + P_{26}},$$

$$P_{39} = \frac{-P_{28}}{P_{24} + P_{26}}, P_{40} = \frac{-P_{29}}{P_{30}}, P_{41} = \frac{-P_{31}}{P_{30}},$$

$$P_{42} = \frac{-P_{32}}{P_{30}}, P_{43} = \frac{-P_{33}}{P_{34}}, P_{44} = \frac{-P_{35}}{P_{34}}, P_{45} = \frac{-P_{36}}{P_{34}},$$

$$P_{46} = \frac{P_{42} - P_{39}}{P_{40} - P_{37}}, P_{47} = \frac{P_{38} - P_{41}}{P_{40} - P_{37}}, P_{48} = \frac{P_{45} - P_{42}}{P_{43} - P_{40}},$$

$$P_{49} = \frac{P_{41} - P_{44}}{P_{43} - P_{40}}, P_{50} = \frac{P_{49} - P_{47}}{P_{48} - P_{46}},$$

$$P_{51} = P_{49} - P_{48}P_{50}, P_{52} = P_{43}P_{51} + P_{44} + P_{45}P_{50},$$

$$P_{53} = P_{24}P_{52} - (P_{22} + P_{51}P_{23}),$$

$$P_{54} = P_{18} + P_{16} + P_{19}P_{50},$$

$$P_{55} = P_{17}\lambda \log\lambda + P_{18}\lambda + \frac{P_{16}}{\lambda} + \frac{P_{19}P_{50}}{\lambda},$$